

Ether Phospholipid-AZT Conjugates Possessing Anti-HIV and Antitumor Cell Activity. Synthesis, Conformational Analysis, and Study of Their Thermal Effects on Membrane Bilayers

Thomas Mavromoustakos,^{*,†} Theodora Calogeropoulou,[†] Maria Koufaki,[†] Antonios Kolocouris,[†] Ioanna Daliani,[†] Costas Demetzos,[‡] Zhaoxing Meng,[§] Alexandros Makriyannis,[§] Jan Balzarini,[#] and Erik De Clercq[#]

National Hellenic Research Foundation, Institute of Organic and Pharmaceutical Chemistry, Vas. Constantinou 48, 116 35, Athens, Greece, School of Pharmacy, Department of Pharmacognosy, University of Athens, Panepistimioupoli-Zografou GR-15771 Athens, Greece, School of Pharmacy, Department of Molecular and Cell Biology and Institute of Materials Science, University of Connecticut, Storrs, Connecticut 06269, and Rega Institute for Medical Research, Katholieke Universiteit Leuven, B-3000 Leuven, Belgium

Received November 24, 2000

The 1-*O*-hexadecyl-2-*O*-methyl-*sn*-glyceryl phosphodiester AZT **4** and hexadecyl-phosphodiester AZT **5** derivatives were synthesized and found to be active against HIV-1, HIV-2, and tumor cell proliferation. Compared to AZT, compound **4** possessed ca. 10-fold lower *anti*-HIV activity and ca. 10-fold higher *anti*-tumor cell activity. Compound **5** was 10-fold less potent than compound **4** in both biological tests. In an attempt to correlate biological activity of compounds **4** and **5** with structure, their conformational and thermal effects on membrane bilayers were compared using a combination of NMR spectroscopy, computational analysis, and Differential Scanning Calorimetry. The obtained results showed that compound **4** adopts a compact conformation in which the alkyl chain, the 2-methoxyglyceryl functionality, and the methyl group of thymine are in spatial proximity, while analogue **5** possesses a less compact conformation of the nucleoside base and the alkyl chain. The presence of the 2-methoxyglyceryl group in compound **4** may augment its potency by inducing a turn of the alkyl chain stabilized by hydrophobic interactions. The DSC scans show that conjugate **4** affects less effectively the thermotropic properties of model membrane bilayers than compound **5**. This may be attributed to the fact that compound **4** is incorporated in a compact conformation and does not perturb significantly the *trans:gauche* isomerization of the membrane phospholipids. In contrast, conjugate **5** may enter with a less compact conformation and perturb more the membrane bilayers.

Introduction

3'-Azido-3'-deoxythymidine (AZT), initially tested as an anticancer agent, is an inhibitor of HIV-1 reverse transcriptase and the first drug clinically used for the treatment of AIDS.^{1,2} In an attempt to improve the biological profile of AZT, various derivatives of this drug have been synthesized.^{3–5} Alkyl and alkoxy,⁶ aryloxy,^{6,7} and alkyl *rac*-glycero and thioglycero^{8,9} phosphoAZT conjugates have attracted special interest since they can penetrate the membranes of virally infected cells and may be subjected to in situ hydrolysis to the corresponding 5'-nucleotide.⁶ Little is known about the cytotoxic properties of the above-mentioned compounds, while various synthesized alkyl phosphate derivatives of other nucleosides exhibit cytotoxic activity against L1210 cell cultures.¹⁰

Our laboratory has been involved in the design and synthesis of 5'-lipophilic AZT phosphates^{6,7} as well as in the study of their biophysical properties i.e., their conformational properties and interactions with mem-

branes.^{11,12} As a continuation of our efforts to explore the stereoelectronic requirements for optimal effectiveness of the lipid component of ether lipid-AZT conjugates, we report the synthesis of 3'-azido-3'-deoxythymidine 5'-[3-(1-*O*-hexadecyl-2-*O*-methyl-*sn*-glyceryl) phosphate] (**4**) and the evaluation of its antiviral and *anti*-tumor cell activity. In an attempt to correlate biological activity with structure, the conformational properties and the effects on membrane bilayers of the alkylglyceryl phosphate AZT conjugate **4** and the less potent alkyl phosphate AZT conjugate **5** which is devoid of the glycerol backbone were compared (Figure 1).

The conformational properties of **4** and **5** were explored using computational analysis coupled with experimental NOE data and their thermal effects on phospholipid bilayers were studied using Differential Scanning Calorimetry.

Results and Discussion

Chemistry. 3'-Azido-3'-deoxythymidine 5'-[3-(1-*O*-hexadecyl-2-*O*-methyl-*sn*-glyceryl) phosphate] (**4**) was synthesized according to Scheme 1. 1-Hexadecyl-2-methyl-*sn*-glycerol (**1**) was prepared from the 2,3-isopropylidene-L-glyceric acid methyl ester according to the procedure described by Bhatia and Hajdu¹⁴ with modifications in the last two steps. Specifically, the alkylation at position *sn*-1 was accomplished by treat-

* To whom correspondence should be addressed. Tel: +30-1-7273869. Fax: +30-1-7273872, +30-1-7273831. E-mail: tmavro@cie.gr.

[†] National Hellenic Research Foundation, Institute of Organic and Pharmaceutical Chemistry.

[‡] University of Athens

[§] University of Connecticut.

[#] Katholieke Universiteit Leuven.

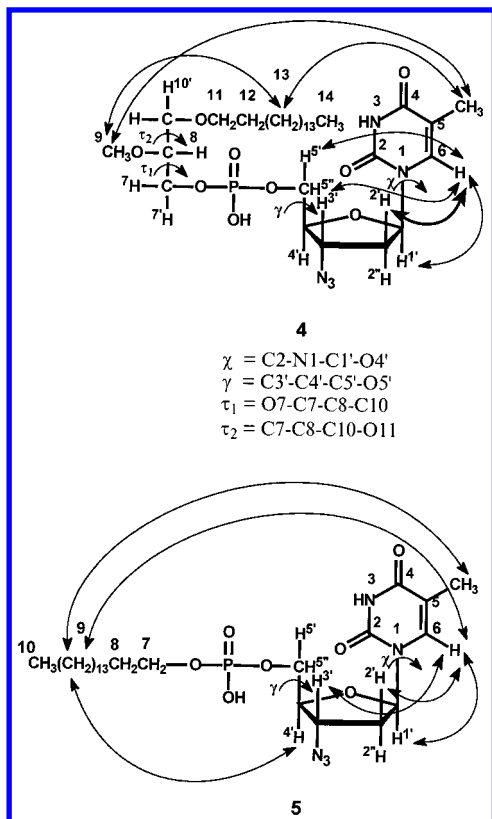


Figure 1. Chemical structures and critical torsion angles for phospholipid AZT conjugates **4** and **5**. In the same figure are shown the most important NOEs observed for compounds **4** and **5** at 298 K.

ment of the alcohol with NaH and 1-hexadecylbromide in toluene at 80–100 °C. Deprotection of the trityl group was performed using HCOOH in ether to yield alcohol **1**. Thus, 1-hexadecyl-2-methyl-*sn*-glycerol (**1**) reacted with excess *o*-chlorophenyl phosphodi-1,2,4-triazolide in pyridine/acetonitrile to afford the corresponding triethylammonium salt **2** after hydrolysis. This, in turn, was coupled with AZT in the presence of the condensing agent 1-mesitylenesulfonyl-3-nitro-1,2,4-triazole (MSNT) to yield the phosphotriester **3** in good yield. Removal of the *o*-chlorophenyl group with tetra-*n*-butylammonium fluoride followed by treatment with Dowex H⁺ yielded the target compound **4**. Compound **5** was synthesized according to previously reported procedures.^{6,7}

Biological Assays. Conjugates **4** and **5** were evaluated against HIV-1 (III_B) and HIV-2 (ROD), and their inhibitory effects were based on suppression of HIV-induced cytopathicity (gland cell formation) in virus-infected human T-lymphocyte CEM cell cultures.^{15,16} The *anti*-HIV activity of compound **4** was about 10-fold lower than that of AZT and 10-fold higher than that of analogue **5** (Table 1), although its cytotoxicity was the highest.

To obtain more detailed information on their mechanism of action, compounds **4** and **5** were examined in thymidine kinase deficient cells in order to evaluate their ability to deliver intracellularly the 5'-nucleotide. To this end, CEM/TK⁻ cells were used which are incapable of phosphorylation and, thus, activation of AZT. As shown in Table 1, compounds **4** and **5** lost their activity against HIV in CEM/TK⁻ cells, suggesting that they do not efficiently deliver AZT monophosphate

(AZT-MP) into the cells but instead are converted to AZT. To further assess this hypothesis, the hydrolytic behavior of the phosphodiester **4** and **5** were examined. Conjugates **4** and **5** (1 mM concentrations) were incubated in the presence of RPMI-1640 and RPMI-1640 containing 10% fetal calf serum (FCS) at 37 °C, and the solutions were analyzed by HPLC and reverse phase thin-layer chromatography. The obtained results show that compounds **4** and **5** were very slowly hydrolyzed only in serum-containing medium to afford AZT, probably through the action of phosphodiesterases and/or phosphatases present in the FCS. On this basis however, we cannot differentiate between the formation of AZT-MP and its rapid conversion to AZT or the direct release of free AZT from the parent compound.

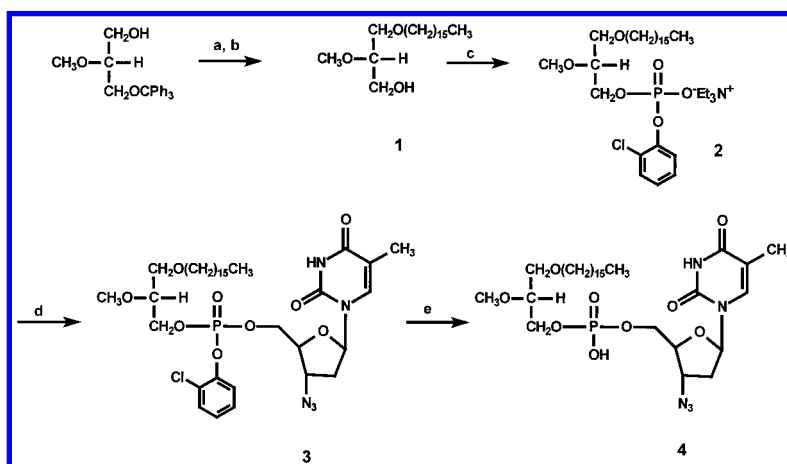
Thus, incubation of conjugate **4** in RPMI-1640 containing 10% FCS resulted to 3.3% and 4.7% hydrolysis after 21 and 45 h, respectively. Similarly, after 45 h incubation 5.9% of compound **5** was hydrolyzed to AZT. AZT-MP was not detected during the experiments.

Compounds **4** and **5** were also evaluated for their inhibitory effects on the proliferation of murine leukemia cells L1210/0 and L1210/TK⁻, murine mammary carcinoma cells FM3A/0, and human T-lymphocyte cells Molt4/C8 and CEM/0 (Table 2). Their inhibitory effect on cell proliferation was expressed as a reduction of the total number of viable tumor cells by 50% upon a 2-day (murine leukemia L1210 and murine mammary carcinoma FM3A) or 3-day (human T-lymphoblast Molt4/C8 and CEM) incubation of the cells at 37 °C.^{15,16}

As compared to AZT and analogue **5**, compound **4** was proved to be approximately 10-fold more potent an inhibitor of tumor cell proliferation. Derivatives **4** and **5** were less active against TK⁻ than L1210/0 cell growth. However, they still retain reasonable activity in contrast to AZT. This is in accordance with the very slow release of AZT that was observed in the hydrolysis experiments described above.

High-Resolution NMR Spectroscopy in Solution. The ¹H NMR spectra of compounds **4** and **5** are shown in Figure 2, and the assignment of ¹H chemical shifts are shown in Table 3. Identification of individual peaks was obtained by peak integration, by analogy with the chemical shift data of 3'-azido-3'-deoxythymidine 5'-phosphate,¹⁷ and with the aid of 2D NMR COSY and NOESY experiments.

In particular, for compound **4**, the COSY spectrum did not allow the differentiation between the closely resonating protons 2' and 2'', and thus, the assignment of these peaks was achieved by the 2D NOESY spectra. The 2' proton was assigned to resonate at 2.24 ppm because of its spatial proximity to 6 proton. The 2'' proton was assigned to resonate at 2.17 ppm since it correlates through space with 1' proton. The most informative observed NOE connectivities were found between the protons: 1'-6 (m = medium), 2'-6 (m), 3'-6 (m), 5'-6 (m), 5CH₃-9 (s = strong), 5CH₃-13 (s), and 9-13 (s) (Figure 1). The 5CH₃-13 proton correlation points to a spatial proximity between the thymine moiety and the alkyl chain. The NOEs found between 5CH₃-9 and 5'-6 reveal a spatial relationship between the glycerol backbone and thymine and give valuable information about the thymine orientation. The NOE observed between 9

Scheme 1^a

^a Reagents and conditions: (a) C₁₆H₃₃Br, NaH, toluene, 100 °C; (b) HCOOH, ether; (c) *o*-chlorophenyl phosphodi-1,2,4-triazolide, pyridine then, Et₃N/H₂O, rt; (d) MSNT, AZT, pyridine, rt; (e) *n*-Bu₄N⁺F⁻, THF/pyridine/H₂O (8:1:1, v/v/v) then, Dowex H⁺.

Table 1. Anti-HIV-1 and Anti-HIV-2 Activity and Cytotoxicity of the Compounds **4** and **5** and AZT in Human T-Lymphocyte (CEM Cells)

compound	EC ₅₀ ^a (μM)			CC ₅₀ ^b (μM) CEM/0
	CEM/0 HIV-1	CEM/0 HIV-2	CEM/TK ⁻ HIV-2	
4	0.065	0.08	>10	34.3 ± 3.0
5	0.58	1.0	>50	161 ± 7
AZT	0.0064	0.006	>100	>500

^a 50% Effective concentration or concentration required to protect CEM cells against the cytopathicity of HIV by 50%. ^b 50% Cytotoxic concentration or concentration required to reduce CEM cell viability by 50%. All data represent average values for at least two separate experiments.

Table 2. Inhibitory Effects of the Compounds **4** and **5** and AZT on the Proliferation of Murine Leukemia Cells (L1210/0, L1210/TK⁻), Murine Mammary Carcinoma Cells (FM3A/0), and Human T-Lymphocyte Cells (Molt4/C8)

compound	IC ₅₀ ^a (μM)			
	L1210/0	L1210/TK ⁻	FM3A/0	Molt4/C8
4	0.98 ± 0.65	33.6 ± 1.2	68.4 ± 7.8	21.4 ± 5.6
5	12.5 ± 3.4	165 ± 3	133 ± 9	144 ± 8
AZT	6.18 ± 3.55	>500	203 ± 173	62.8 ± 23.5

^a 50% Inhibitory concentration or concentration required to inhibit cell growth by 50%. All data represent average values for at least two separate experiments.

and 13 protons indicates an alkyl chain–glycerol backbone spatial relationship.

The same strategy was applied for the assignment of the proton resonances for compound **5** (Figure 1, Table 3). The most important NOE connectivities that determine its conformation were found between protons 1'–6 (m), 2'–6 (m), 3'–6 (m), 4'–9 (s), 5CH₃–9 (s), and 6–9 (m) (Figure 1). These NOEs suggest different conformational properties for compound **5**.

Conformational Analysis. The conformational analysis for AZT derivatives **4** and **5** was carried out using a combination of NMR spectroscopy and computational analysis.

Molecular dynamics using the most important NOE constraints and coupled with minimization algorithms were initially carried out for compounds **4** and **5** to generate a set of 12 families of low energy conformers.¹³ From those conformers only three for compound **4** (Figure 3A–C) and four for compound **5** (Figure 3D–

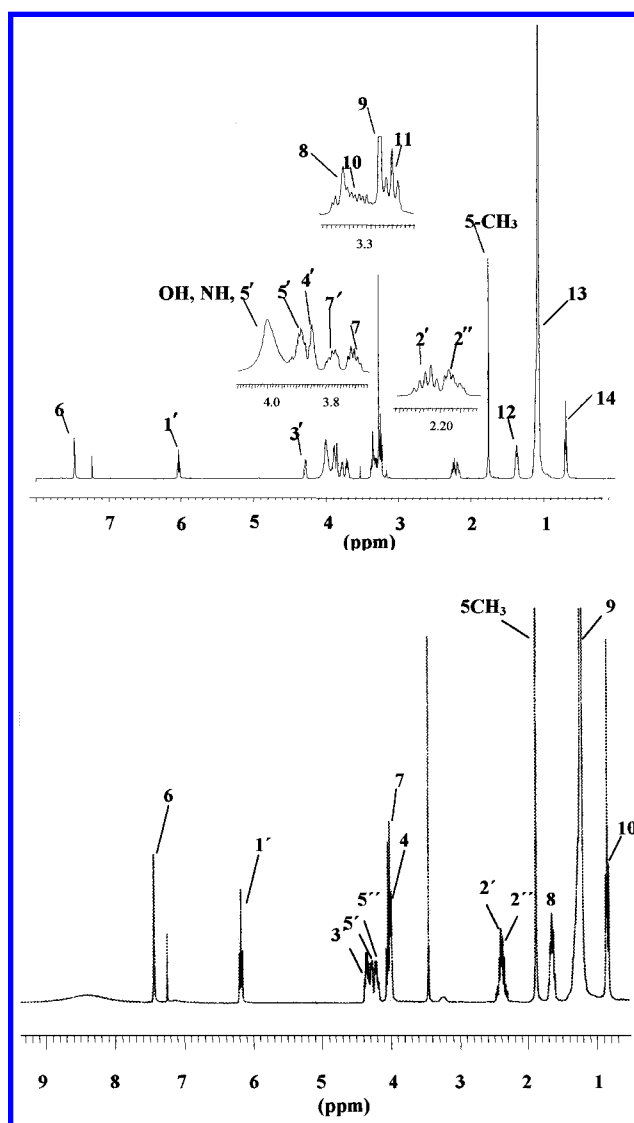


Figure 2. ¹H NMR spectra of AZT derivatives **4** and **5** in CDCl₃ at 298 K.

G) were consistent with NOE data. The conformational characteristics for these conformers in terms of nucleoside moiety, glycerol backbone, and alkyl chain conformation are briefly discussed.

Conformation of Nucleoside Moiety. The confor-

Table 3. ¹H NMR Chemical Shifts (ppm) of Phospholipid AZT Conjugates **4** and **5** Obtained in CDCl₃ Solution at 298 K Using TMS as Internal Reference

compound 4		compound 5	
proton	chemical shift	proton	chemical shift
14	0.70	10	0.75
13	1.08	9	1.11
12	1.38	8	1.56
5-CH ₃	1.76	5-CH ₃	1.78
2'	2.20	2'	2.25
2''	2.24	2''	2.31
11	3.26	7	3.37
9	3.28	4	3.30
10	3.33	5' ^a	4.20
8	3.37	5'' ^a	4.28
7	3.73	3'	4.35
7'	3.78	1'	6.17
4'	3.86	6	7.38
5' ^a	3.90		
5'' ^a	4.01		
3'	4.29		
1'	6.04		
6	7.48		

^a The chemical shifts of these protons can be interchanged.

Table 4. Values of Phase Pretransition and Transition Temperatures (T_m), Half-Width Temperature ($T_{m1/2}$), and Enthalpy Changes (ΔH) of DPPC with or without Compound **4** or **5**

samples	$T_{m1/2}$	T_m	ΔH
DPPC alone	1.0	35.9, 42.3	5.6, 42.8
DPPC + 5 ($x = 0.01$)	1.3	30.9, 40.4	43.4
DPPC + 5 ($x = 0.05$)	1.7	40.2	43.9
DPPC + 5 ($x = 0.1$)	2.0	39.3	42.7
DPPC + 5 ($x = 0.2$)	2.8	36.7	45.9
DPPC + 4 ($x = 0.01$)	1.2	34.2, 41.0	53.4
DPPC + 4 ($x = 0.05$)	1.5	40.8	43.8
DPPC + 4 ($x = 0.10$)	2.3	40.4	46.9
DPPC + 4 ($x = 0.20$)	2.4	39.5	50.4

mation of the nucleoside moiety for molecules **4** and **5** was determined by studying the puckering of the sugar ring, the geometry of the glycosidic linkage (defined by the χ dihedral angle C2-N1-C1'-O4'), and the rotation about the exocyclic C4'-C5' bond (defined by the γ dihedral angle C3'-C4'-C5'-O5').

H1' resonances of the ether phospholipid AZT conjugates **4** and **5** appeared as triplets ($J = 6.4$ Hz for compound **4** and 6.0 Hz for compound **5**). A similar spectral feature was observed for the free AZT nucleoside and indicates a predominant C2'-endo solution conformation of the sugar ring. The absence of a NOE between H2''-H4' also confirms a C2'-endo deoxyribose conformation which is further supported by the H6-H2' NOE correlation.¹⁸⁻²⁰

The heterocyclic base of compound **4** was found to adopt an anti orientation around the glycosidic bond. An anti orientation is characterized by χ torsion angle values varying between -170° and -90° .²⁰ The NOEs between protons 5CH₃-9 and 5'-6 support this orientation. For compound **5** no dipolar correlation was observed between protons 5'-6. This suggests a more flexible rotation about C1'-N1 bond which allows the thymine base to move easily between an anti and a syn orientation (torsion angle values varying between 50° and 90°). The results of the dynamics calculations reflect this flexibility as shown in the represented low energy conformers (Figure 3D-G). The conformation around torsion angle γ was found to be (+)gauche-(-)gauche

or (+)gauche-trans for low energy conformers of compounds **4** and **5**.

Conformation of the Glycerol Backbone and Alkyl Chain. The conformation of the glycerol backbone for compound **4** was determined by the torsion angles τ_1 and τ_2 . Six rotamers with staggered conformations about the two carbon-carbon glycerol bonds are possible. Torsion angles τ_1 and τ_2 were found to be (+)gauche-trans, trans-(-)gauche, (+)gauche-(-)gauche, (+)gauche-trans, or trans-(-)gauche, (+)gauche-(-)gauche.

The combination of dynamics simulation and NOE spectroscopy revealed an isomerization of an extended all-trans alkyl chain conformer to several low energy conformers that include trans-gauche orientations around carbon-carbon bonds. The isomerization of the alkyl chain creates an energetically favorable turn of the chain and establishes a spatial proximity between the alkyl chain, the glycerol backbone, and the methyl group of AZT thymine as shown in low energy conformers of Figure 3A-C. This stabilizing effect can explain the observed compact anti orientation of thymine base in compound **4** compared with derivative **5** which adopts a more random conformation of nucleoside and alkyl chain groups (Figure 3D-G).

In conclusion, the obtained results showed that the nucleoside and alkyl chain moieties adopt a more compact conformation in compound **4** than that of compound **5**. This higher flexibility of compound **5** does not allow a unique family of low energy conformers that accounts for all observed NOEs.

Differential Scanning Calorimetry (DSC). To examine if the observed conformational differences between compounds **4** and **5** may consequently induce any differences in their physicochemical interactions with lipid bilayers, DSC was applied. The DSC traces of DPPC bilayers without or with either compounds **4** or **5** are shown in Figure 4.

Fully hydrated DPPC phospholipids spontaneously form bilayers whose dynamic and thermotropic properties have been extensively studied by various biophysical methods.^{21,22} These methods showed that these bilayers exist in the gel phase at temperatures lower than 35°C and in the liquid crystalline phase at temperatures higher than 42°C . The transition is accompanied by several structural changes in the lipid molecules as well as alterations in the bilayer geometry. The most prominent feature during the transition is the trans-gauche isomerization taking place in the acyl chain conformation. The average number of gauche conformers indicates the effective fluidity, which depends not only on the temperature but also on perturbations due to the presence of an additive intercalating between the phospholipids.

The addition of $x = 0.01$ (1%-molar ratio) of the more active analogue **4** does not cause any significant change in the main phase transition but broadens the pretransition temperature. In contrast, the presence of the less active analogue **5** causes lowering of the main phase transition temperature by 0.6 K relative to compound **4**. At $x = 0.05$, the presence of either compound in DPPC bilayers abolishes the pretransition temperature, but the presence of compound **5** still causes more lowering of the main phase transition temperature by 0.6 K in

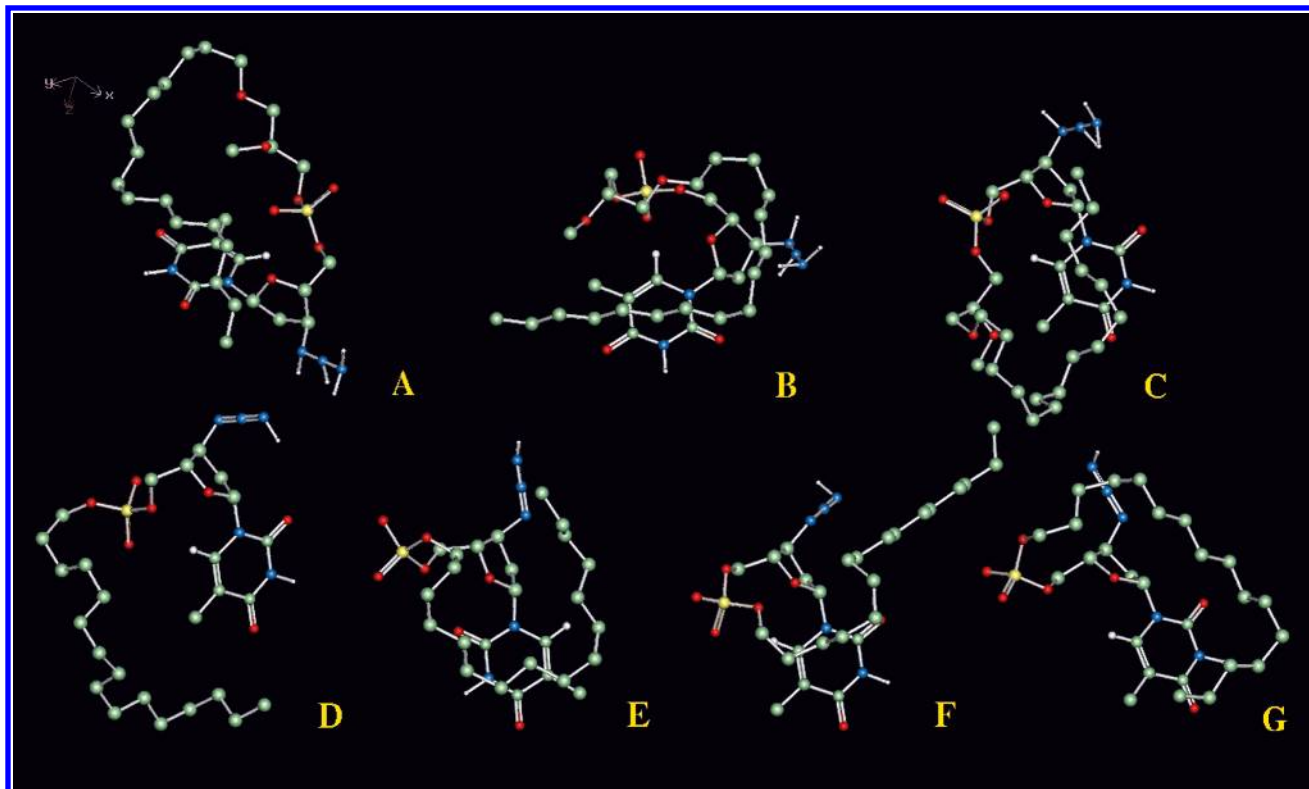


Figure 3. Low energy conformations of alkylglycerophospholipid AZT derivative **4** (A–C) and alkylphospholipid AZT derivative **5** (D–G) resulting from the combined use of NMR spectroscopy and computational chemistry. Hydrogens are omitted for better representation.

comparison to compound **4**. At high concentrations of $x = 0.10$ and $x = 0.20$ both compounds broaden the phase transition and cause a lowering of the phase transition temperature, but the effects of compound **5** are clearly far more pronounced than those of compound **4** as it is depicted from the values of diagnostic parameters $T_{m1/2}$ and T_m . Higher ΔH values were observed for derivative **4** as it is expected, because it probably fits better in the membrane bilayers and it does not perturb the cooperativity of the lipid chains.

The obtained results suggest that the less active analogue **5** perturbs more membrane bilayers probably because of its adopted more flexible conformation. The more active compound **4** which adopts a compact conformation may fit better into the membrane bilayer and causes less significant effects.

It appears that the use of DSC may increase our understanding of a possible relationship between the conformational properties of the phospholipid AZT conjugates and their membrane interactions.

Conclusion

The synthetic AZT derivative **4** was found to possess both *anti*-HIV and *anti*-tumor cell activities. Interestingly, conjugate **5** which is devoid of glycerol backbone possesses 10-fold less activity as anticancer and HIV agent than compound **4**. The two molecules differ not only in their biological profile but also in their conformational properties and thermal effects on membrane bilayers. Compound **4** prefers a compact conformation in which the alkyl chain, the 2-methoxyglyceryl group, and the 5-CH₃ are in close contact so as to favor hydrophobic interactions, while compound **5** adopts a less defined conformation with respect to the nucleoside

moiety and alkyl chain. Thus, it seems that 2-methoxyglycerol backbone stabilizes the compact conformation observed for compound **4**. Such a compact conformation may be related to its way of entering the degree of penetration in the membrane bilayers and the less efficient perturbation compared to **5**. It remains to be seen whether novel phospholipid AZT analogues that adopt a compact conformation will possess improved *anti*-cancer and *anti*-HIV properties.

Experimental Section

Chemistry. All reactions were carried out under scrupulously dry conditions. NMR spectra of all the intermediate compounds were recorded on a Bruker AC 300 spectrometer operating at 300 MHz for ¹H and 121.44 MHz for ³¹P. ¹H NMR spectra are reported in units of δ with CHCl₃ resonance at 7.24 ppm used as the chemical shift resonance. ³¹P NMR spectra are reported in units of δ relative to 85% H₃PO₄ used as an external standard. Silica gel plates (Merck F254) were used for thin-layer chromatography. Chromatographic purification was performed with silica gel (200–400 mesh). The microanalysis of compound **4** was carried out by the Service Central de Microanalyse (CNRS), France. HPLC data were recorded using a Waters quaternary system.

1-Hexadecyl-2-methyl-3-(triphenylmethyl)-*sn*-glycerol. To a slurry of NaH (0.132 g, 5.5 mmol, washed twice with anhydrous hexane) in toluene (4 mL) was added at 0 °C a solution of 2-methyl-3-(triphenylmethyl) glycerol (0.950 g, 2.75 mmol) in toluene (4 mL). The resulting mixture was stirred at 0 °C for 0.5 h, and then 1-bromohexadecane (1.049 g, 3.44 mmol) and KI (0.057 g, 0.344 mmol) were added. The resulting mixture was stirred at 100 °C for 12 h. The reaction was quenched at 0 °C, by addition of MeOH (1 mL). The mixture was diluted with ether and washed with H₂O and brine. The organic layer was dried (Na₂SO₄), and the solvent was evaporated in vacuo to afford the desired product in 82% yield after purification of the residue by flash column chro-

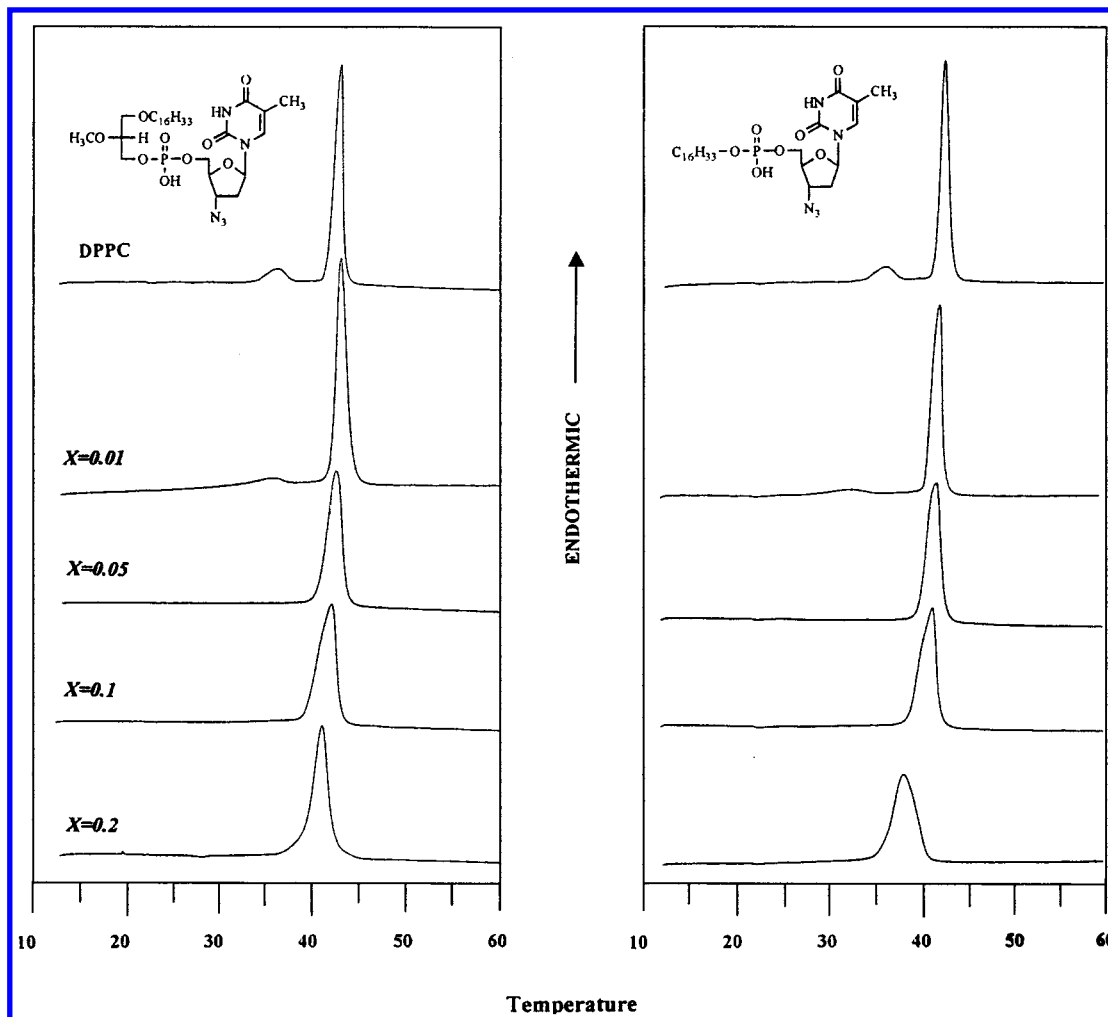


Figure 4. DSC scans of DPPC bilayers alone or with incorporation of phospholipid AZT derivative **4** or **5**.

matography using a mixture of petroleum ether (40–60 °C)/ethyl acetate (95:5) as eluting solvent. Spectral data and optical rotation were in accordance with those reported in ref 14.

1-Hexadecyl-2-methyl-*sn*-glycerol (1). A solution of 1-hexadecyl-2-methyl-3-(triphenylmethyl)-*sn*-glycerol (1.2 g, 2.2 mmol) in a mixture of formic acid (90%) (4.4 mL) and diethyl ether (4.4 mL) was stirred at room temperature for 3 h. Addition of ether was followed by extraction with saturated aqueous NaHCO_3 , H_2O , and brine. The solvent was evaporated in vacuo, the resulting solid was dissolved in methanol (25 mL), and K_2CO_3 (6.6 mmol) was added. The reaction mixture was stirred until TLC showed the formate esters were completely hydrolyzed. The K_2CO_3 was filtered off; the filtrate was diluted with ether and washed with saturated aqueous NH_4Cl , H_2O , and brine. The organic layer was dried (Na_2SO_4), and the solvent was evaporated *in vacuo*. After purification of the residue by flash column chromatography using petroleum ether (40–60 °C)/ethyl acetate (75:25) as eluting solvent, the desired product **1** was afforded in 92% yield. Spectral data and optical rotation were in accordance with those reported in ref 14.

2-Chlorophenyl 5'-(3'-azido-3'-deoxythymidinyl) 1-Hexadecyl-2-methoxy-*sn*-glyceryl Phosphate (3). To an ice-cooled solution of *o*-chlorophenyl phosphodichloridate (0.17 mL, 1 mmol) in acetonitrile (4 mL) were sequentially added 1,2,4-triazole (0.155 g, 2.2 mmol) and triethylamine (0.3 mL), and the mixture was stirred at room temperature for 30 min. 1-Hexadecyl-2-methyl-*sn*-glycerol (**1**) (0.152 g, 0.5 mmol) in pyridine (4 mL) and after a period of 45 min triethylamine (0.35 mL) and water (0.1 mL) were added. The mixture was stirred for 10 min, and addition of saturated aqueous NaHCO_3

was followed by extraction with dichloromethane. The organic phase was dried (Na_2SO_4) and evaporated in vacuo. The resulting (*o*-chlorophenyl)phosphatidic acid triethylammonium salt **2** was used without further purification for the next step.

Compound **2** was dissolved in pyridine (2.5 mL) and 1-(mesitylenesulfonyl)-3-nitro-1,2,4-triazole (MSNT) (0.180 g, 0.67 mmol) and AZT (0.150 g, 0.56 mmol) was added. After stirring at room temperature for 12 h, aqueous NaHCO_3 was added, and the mixture was extracted with dichloromethane. The organic phase was washed with water and was saturated with aqueous NaCl and dried over Na_2SO_4 . The residue was purified by column chromatography using a gradient of dichloromethane/acetone (90:10–85:15) to afford 0.270 g (71.8%) of the desired product **3**. ^1H NMR (300 MHz) δ 8.35 (bs, 1H, NH), 7.50–7.05 (m, 5H, ArH, H6), 6.22 (t, $J = 6.5$ Hz, 1H), 4.51–4.07 (m, 6H), 3.55–3.34 (m, 8H), 2.49–2.21 (m, 2H), 1.88 (s, 3H), 1.7–1.45 (m, 2H), 1.30–1.15 (m, 26 H), 0.88 (t, $J = 6.8$ Hz, 3H); ^{31}P NMR (121 MHz) δ -8.22, -8.29.

3'-Azido-3'-deoxythymidine 5'-[3-(1-*O*-Hexadecyl-2-*O*-methyl-*sn*-glyceryl) Phosphate] (4). Tetra-*n*-butylammonium fluoride (1 mmol 1M in THF) was added to a solution of 2-chlorophenyl 5'-(3'-azido-2'-deoxythymidinyl) 1-hexadecyl-2-methoxy-glyceryl phosphate (**3**) (0.250 g, 0.33 mmol) in 3.5 mL of a THF–pyridine–water (8:1:1 v/v/v) mixture. The mixture was then stirred at room temperature for 5 h, worked up by addition of saturated aqueous NaHCO_3 , and extracted with dichloromethane. The organic phase was evaporated, and the residue was purified by column chromatography using the dichloromethane/methanol gradient (95:5–50:50 v/v). The appropriate fractions were concentrated and treated with

DOWEX 50WX8 (H⁺) in methanol to afford the final phosphodiester **4** (0.147 g, 68%). ³¹P NMR δ -1.85. Anal. (C₃₀H₅₄N₅O₈P·H₂O) C, H.

Stability of Compounds 4 and 5. Conjugates **4** and **5** (1 mM concentrations) were incubated in the presence of RPMI-1640 culture medium and RPMI-1640 culture medium containing 10% fetal calf serum. The solutions were monitored by HPLC, using an ODS10 column, an eluent of water/acetonitrile, and a linear gradient from 100% water to 20% water at 30 min, with a flow rate of 2 mL min⁻¹ and detection by UV at 265 nm. Reverse-phase thin-layer chromatography (RP-18 TLC plates and eluent system of water/acetonitrile 1:1) was also used for monitoring the solutions. For identification of the possible hydrolysis products AZT-MP, hexadecyl monophosphate, and 1-*O*-hexadecyl-2-*O*-methyl-*sn*-glycerol monophosphate were synthesized and used as standards.

NMR Spectroscopy. NMR spectra were obtained using Bruker 300, 400, and 500 MHz instruments. COSY and NOESY 2D-NMR experiments were performed using pulse sequences and phase-cycling routines provided in the Bruker library of pulse programs. Data processing were performed using Bruker software packages.

¹H NMR spectra for compounds **4** and **5** were recorded using the following acquisition parameters: pulse width (PW) 6.0 μs, (SW) 6023 Hz, data size (TD) 16K, recycling delay (RD) 1.0 s, number of transients (NS) 16, and digital resolution 0.37 Hz/pt. The acquisition parameters used for the ¹H-¹H correlation COSY spectra were as follows: recycling delay (D1) 2.0 s, D0 increment 3 μs, and spectral width in F2 2512.56 Hz and in F1 1256.28 Hz. The data sizes were as follows: 1024 and 128 data points in F1 and F2, respectively; the data were zero-filled in F1 to 256 data points prior to 2D Fourier transformation giving digital resolution 9.81 Hz/pt. The spectrum was processed using a sine-bell window function both in F1 and F2 (WDW=S) and was symmetrized about the diagonal.

2D ¹H-¹H nuclear Overhauser enhancement (NOESY) spectra were recorded using the acquisition parameters: D1 = 3s, D0 = 3 μs, and SW in F2 2702.70 and 1351.35 Hz in F1. The data sizes were as follows: 1024 and 512 data points in F1 and F2, respectively; the data were zero-filled in F1 to 1024 data points prior to 2D Fourier transformation giving digital resolution 2.64 Hz/pt. The optimum mixing time (D9) was found to be 0.5 s. The spectrum was processed as in the COSY experiment.

Molecular Modeling. Computer calculations were performed on a Silicon Graphics O2 using the QUANTA software package. Molecular mechanics calculations were carried out using the CHARMM force field. The conformational energy of lipid-AZT conjugate **4** and **5** were first minimized with conjugate gradient and then with Newton-Raphson algorithms, using an energy gradient tolerance of 0.01 kcal mol⁻¹ Å⁻¹ to reach a local minimum. These structures were subjected to an unrestrained molecular dynamics simulation at 1000 K for 300 ps (ε = 1). Conformations were sampled every 1 ps during the simulation, resulting in 300 randomized structures which were subjected to restrained energy minimization using 1000 steps of conjugate gradient algorithm. The upper bound distances used were 3.0 and 3.5 Å for strong and medium NOE correlations correspondingly. After cluster analysis using a torsion angle threshold of 83°, 12 family structures were selected. The obtained low energy structures of each cluster were further minimized to reach local minima. Three conformers assigned as A-C for compound **5** (Figure 3A-C) support the observed NOE between 9CH₃-13, and four conformers (Figure 3D-G) for compound **4** represent low energy structures consistent with the NMR data.

Differential Scanning Calorimetry. Appropriate amounts of the phospholipid with or without AZT derivative **4** or **5** were dissolved in spectroscopic grade chloroform. The solvent was then evaporated under vacuum (0.1 mmHg) at temperature above the transition temperature. For measurements this dry residue was dispersed in appropriate amounts of bi-distilled water by vortexing. The samples (ca. 5 mg) were sealed into

stainless steel capsules obtained from Perkin-Elmer. Thermograms were obtained on a Perkin-Elmer DSC-7 calorimeter. Prior to scanning the samples were held above their phase transition temperature for 1–2 min to ensure equilibration. All samples were scanned at least twice until identical thermograms were obtained using a scanning rate of 2.5 °C/min. The temperature scale of the calorimeter was calibrated using indium (T_m = 156.6 °C) as a standard sample.

Acknowledgment. This work was supported by grants from the European Commission and from the Belgian Government (95/5). The excellent technical help of Mrs. Ann Absillis and Lizette van Berchelaen was highly appreciated.

References

- (1) Mitsuya, H.; Weinhold, K. J.; Furman, P. A.; St. Clair, M. H.; Nusinoff-Lehrman, S.; Gallo, R. C.; Bolognesi, D.; Barry, D. W.; Broder S. 3'-Azido-3'-deoxythymidine (BWA509U): an antiviral agent that inhibits the infectivity and cytopathic effect on human T-lymphotropic virus type III/lymphadenopathy-associated virus in vitro. *Proc. Natl. Acad. Sci. U.S.A.* **1985**, *82*, 7096–7100.
- (2) Fischl, M. A.; Richman, D. D.; Grieco, M. H.; Gottlieb, M. S.; Volberding, P. A.; Laskin, O. L.; Leedom, J. M.; Groopman, J. E.; Mildvan, D.; Schooley, R. T.; Jackson, G. G.; Durack, D. T.; King, D. The efficacy of Complex - A double-blind, placebo-controlled trial. *N. Engl. J. Med.* **1987**, *317*, 185–191.
- (3) Van Wijk, G. M. T.; Hostetler, K. Y.; Kroneman, E.; Richman, D. D.; Sridhar, C. N.; Kumar, R.; van der Bosch, H. Synthesis and antiviral activity of 3'-azido-3'-deoxythymidine triphosphate distearoylglycerol: a novel phospholipid conjugate of the anti-HIV agent AZT. *Chem. Phys. Lipids* **1994**, *70*, 213–222.
- (4) Perigaud, C.; Girardet, J.-L.; Gosselin, G.; Imbach, J.-L. In *Advances in Antiviral Drug Design*; De Clercq, E., Ed.; 1995; Vol. 2, pp 167–172.
- (5) Jones, R. J.; Bischofberger, N. Nucleotide prodrugs. *Antiviral Res.* **1995**, *27*, 1–17.
- (6) Calogeropoulou, T.; Koufaki, M.; Tsotinis, A.; Balzarini, J.; De Clercq, E.; Makriyannis, A. Synthesis and anti-HIV evaluation of alkyl and alkoxyethyl phosphotriester AZT derivatives. *Antiviral Chem. Chemother.* **1995**, *6*, 43–49.
- (7) Tsotinis, A.; Calogeropoulou, T.; Koufaki, M.; Souli, C.; Balzarini, J.; De Clercq, E.; Makriyannis, A. Synthesis and antiretroviral evaluation of new alkoxy and aryloxy phosphate derivatives of 3'-azido-3'-deoxythymidine. *J. Med. Chem.* **1996**, *39*, 3418–3422.
- (8) Piantadosi, C.; Marasco Jr., C. J.; Morris-Natschke, S. L.; Meyer, K. L.; Gumus, F.; Surles, J. R.; Ishaq, K. S.; Kucera, L. S.; Iyer, N.; Wallen, C. A.; Piantadosi, S.; Modest, E. J. Synthesis and evaluation of novel ether lipid nucleoside conjugates for anti-HIV-1 activity. *J. Med. Chem.* **1991**, *34*, 1408–1414.
- (9) Hong, C. I.; Nechaev, A.; Kiritsis, A. J.; Vig, R.; West, C. R.; Manouilov, K. K.; Chu, C. K. Nucleoside conjugates. 15. Synthesis and biological activity of anti-HIV nucleoside conjugates of ether and thioether phospholipids. *J. Med. Chem.* **1996**, *39*, 1771–1777.
- (10) Brachwitz, H.; Bergmann, J.; Thomas, Y.; Berdel, W. E.; Langen, P.; Wolny, T. Synthesis and cytostatic evaluation of cytidine and adenosine-5-hexadecyl phosphate and their phosphonate analogues. *Chem. Phys. Lipids* **1997**, *90*, 143–149.
- (11) Mavromoustakos, T.; Theodoropoulou, E.; Yang, D. P.; Lin, S. Y.; Koufaki, M.; Makriyannis, A. The conformational properties of the antineoplastic ether lipid 1-thiohexadecyl-2-*O*-methyl-*S*-glycero-3-phosphocholine. *Chem. Phys. Lipids* **1996**, *84*, 21–34.
- (12) Koufaki, M.; Calogeropoulou, T.; Mavromoustakos, T.; Theodoropoulou, E.; Tsotinis, A.; Makriyannis, A. Synthesis of ²H-labeled alkoxyethyl phosphodiester (AZT) derivatives for solid-state ²H NMR studies. *J. Heterocyclic Chem.* **1996**, *33*, 619–622.
- (13) Howard, A. E.; Kollman, P. A. An analysis of current methodologies for conformational searching of complex molecules. *J. Med. Chem.* **1988**, *31*, 1669–1675.
- (14) Bhatia, S. K.; Hajdu, J. Stereospecific synthesis of ether an thioether phospholipids. The use of L-glyceric acid as a chiral phospholipid precursor. *J. Org. Chem.* **1988**, *53*, 5034–5039.
- (15) Popovic, M.; Sarngadharan, M. C.; Read, E.; Gallo, R. C. Detection, isolation, and continuous production of cytopathic retroviruses (HTLV-III) from patients with AIDS and pre-AIDS. *Science* **1984**, *224*, 497–500.
- (16) Balzarini, J.; Naesens, L.; Slachmuylders, J.; Niphuis, H.; Rosenberg, I.; Holy, A.; Schellekens, H.; De Clercq, E. 9-(2-Phosphonylmethoxyethyl)adenine (PMEA) effectively inhibits retrovirus replication in vitro and simian immunodeficiency virus-infection in rhesus-monkeys. *AIDS* **1991**, *5*, 21–28.
- (17) Swapna, G. V. T.; Jagannadh, B.; Gurjar M. K.; Kunwar, A. C. NMR investigation on the structure and conformation of 3'-azido-

- 2',3'-dideoxyribosylthymine (AZT), an inhibitor of the HIV (AIDS virus). *Biochem. Biophys. Res. Commun.* **1989**, *164*, 1086–1092.
- (18) Herzyk, P.; Beveridge, A.; Neidle, S. Conformational properties of 3'-azido-3'-deoxythymidine (AZT), an inhibitor of HIV reverse transcriptase. *Biochem. Biophys. Res. Commun.* **1987**, *145*, 1356–1361.
- (19) Meier, C.; Neumann, J.-M.; Andre, F.; Henin Y.; Huynh-Dinh, T. *O*-Alkyl-5',5'-dinucleoside phosphates as prodrugs of 3'-azidothymidine and cordycepin. *J. Med. Chem.* **1992**, *35*, 7300–7308.
- (20) Van Roey, P.; Salerno, J. M.; Chu, C. K.; Schinazi, R. F. Correlation between preferred sugar ring conformation and activity of nucleoside analogues against human immunodeficiency virus. *Proc. Natl. Acad. Sci. U.S.A.* **1989**, *86*, 3929–3933.
- (21) Hinz H. J.; Sturtevant, J. M.; Calorimetric Studies of Dilute Aqueous Suspensions of Bilayers Formed from Synthetic L- α -Lecithins *J. Biol. Chem.* **1972**, *10*, 6071–6075.
- (22) Witterbort, R. J.; Blume, A.; Huang, T. H.; Das Gupta, S. K.; Griffin, R. G.; 1982. Carbon-13 nuclear magnetic resonance of the lecithin gel to liquid-crystalline phase transition. *Biochemistry* **1982**, *21*, 3487–3502.

JM001121C